

UNCLASSIFIED

Defense Technical Information Center
Compilation Part Notice

ADP013283

TITLE: Normal-to-Plane Magnetoresistance of Single Crystalline Refractory Metal Nanostructures

DISTRIBUTION: Approved for public release, distribution unlimited
Availability: Hard copy only.

This paper is part of the following report:

TITLE: Nanostructures: Physics and Technology International Symposium [9th], St. Petersburg, Russia, June 18-22, 2001 Proceedings

To order the complete compilation report, use: ADA408025

The component part is provided here to allow users access to individually authored sections of proceedings, annals, symposia, etc. However, the component should be considered within the context of the overall compilation report and not as a stand-alone technical report.

The following component part numbers comprise the compilation report:

ADP013147 thru ADP013308

UNCLASSIFIED

Normal-to-plane magnetoresistance of single crystalline refractory metal nanostructures

G. M. Mikhailov[†], *I. V. Malikov*[†], *A. V. Chernykh*[†], *L. A. Fomin*[†], *P. Joyez*[‡],
H. Pothier[‡], *D. Esteve*[‡] and *E. Olsson*[§]

[†] IMT RAS, 142432 Chernogolovka, Russia

[‡] SPEC-CEA Saclay, France

[§] Angstrom Laboratory, Uppsala University, Sweden

Abstract. We have performed normal-to-plane magnetotransport measurements in single crystalline (100) W and Mo nanostructures down to 1.5 K. Fabricated nanostructures possess large mean free path due to their bulk crystalline perfection and low surface roughness. Under these conditions electrons scatter only on the boundaries of nanostructures and may travel long distance without scattering. We found that in this regime the normal-to-plane magnetoresistance of planar metallic nanostructures exhibit specific for ballistic transport attributes such as transverse magnetic focusing, suppression of Hall resistance (quenching Hall effect) and negative bend resistance at moderate magnetic fields.

Introduction

Investigation of novel planar heteroepitaxial metallic structures (thin films and nanostructures) attract much attention as they demonstrate new properties. Because of high crystalline quality and low roughness of their interface conducting electrons may travel long distance without scattering in these structures. Both ballistic and waveguiding properties become apparent. Electron momentum dissipation is driven by electron scattering on the irregularities of the boundaries. In this regime the electron current is mainly formed by grazing electron flow. Normal-to-plane magnetic field modifies their trajectories and the edge states (skipping orbits) are formed. In the following, we present for the first time the results of magnetoresistance investigation of refractory metal single crystalline planar nanostructures under conditions, when electron mean free path is comparable or superior the structure dimensions.

1. Experimental set-up and characterizations

Fabrication of the structures has been performed using pulse laser epitaxy of refractory metals, namely Mo (100) and W(100), on r-plane sapphire. Grown films possess high crystalline quality and low interface roughness. In Figure 1(a) we present transmission electron microscope image of Mo (100) thin foil that demonstrate atomic layers of substrate and metallic film. As electron scattering is driven by boundaries irregularities, we have been investigated the film morphology using scanning atomic force microscope (P47-Solvent-NT-MDT). Root mean square (r.m.s.) of roughness amplitude has been found from larger than one by one micrometer topography scan. It equals 0.216 and 0.14 nm for Mo film surface and substrate, respectively. To characterize scattering properties of the rough surface the power spectrum of surface fluctuation and mean scattering wave vector have been building up. They are shown in Fig. 1(b) and (c). As can be seen in the latter, both

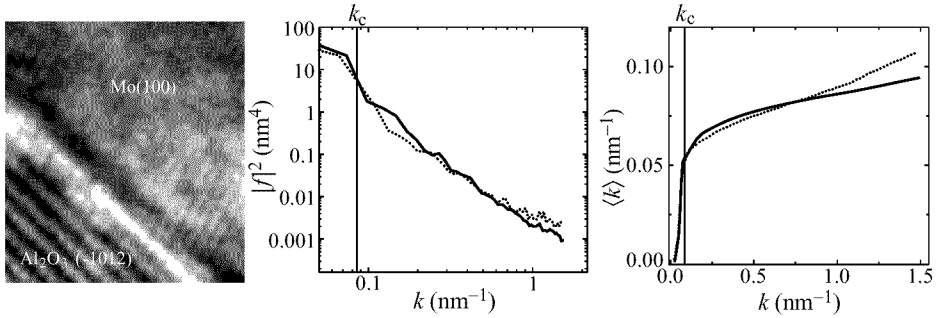


Fig. 1. Transmission electron microscope image of thin foil of Mo(100) films (a), power spectrum (b) and mean transfer wave vector (c) for surface fluctuation of Mo(100) surface (solid line) and substrate (dotted line).

small ($< k_c/k_F$) and large ($\gg k_c/k_F$) angle electron scattering contributes to electron momentum dissipation, where correlating wave vector is equaled to $k_c \approx 0.085 \text{ nm}^{-1}$ both for Mo film and substrate surfaces and k_F is Fermi wave vector. These well-characterized single crystalline films have been used for fabrication of single crystalline nanostructures with the help of subtractive electron lithography, Al nanomask developing and low energy ion milling. The resistance was measured by conventional ac techniques at 4.2 K, with an applied magnetic field up to 8 T directed perpendicular to the sample plane. The effective mean free path (EMFP) of electrons, estimated from the bridge-resistance ratio at $T = 295$ and 4.2 K, is found to be dependent on the film thickness. At low temperature, it is approximately an order of magnitude larger the film thickness. The mean cyclotron radius is estimated as $r_L = 3 (T\mu\text{m})/B(\text{T})$.

1.1. Transverse magnetic focusing

To perform focusing experiment we fabricated planar Mo (100) structure that depicted in Fig. 2 (left) together with electric set-up. Semi-plane of 200 nm thickness is connected to the potential (3, 4) and current leads (1 or 2) in one side. Counterpart current lead

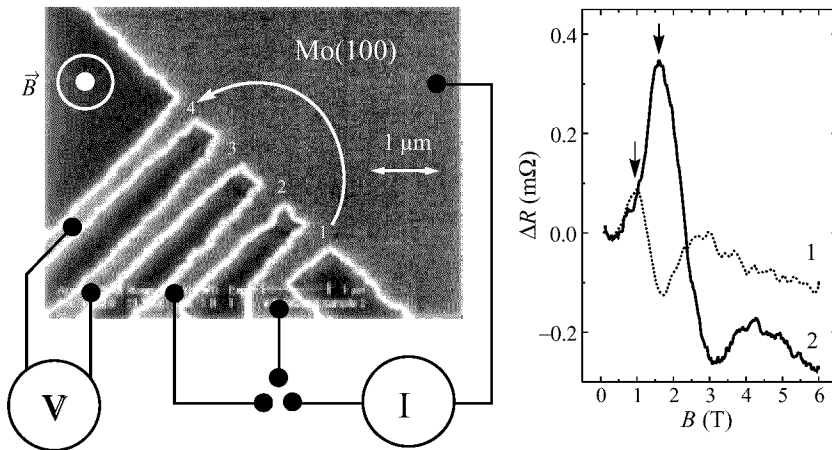


Fig. 2. The Mo (100) structure and electric set-up (left) and antisymmetric magnetoresistance for the lead 1 (dotted curve) or the lead 2 (solid curve) as an injecting electrode.

(schematically shown) is attached to the opposite side of the semi-plane. The current lead (1 or 2) serves as an injecting electrode, while potential leads 4 or 3 as an accepting electrode. Considering further isotropic electron spectrum for simplicity, we show in Fig. 2 an electron trajectory bended by applied magnetic field that close the injecting electrode 1 and accepting electrode 4 (positive lead of potentiometer), the cyclotron radius being twice smaller than the inter-electrode distance. By increasing of magnetic field we scan electron focusing point toward the injecting electrode. At some its meaning the bended electron trajectory points the lead 3 (negative lead of potentiometer). As the result we found in antisymmetric magnetoresistance ($\Delta R = R(B) - R(-B)$) positive and negative peaks, respectively (dotted curve in Fig. 2, right). For the lead 2 as an injecting electrode we found the same dependence but extended toward higher magnetic field in about two times (solid curve). Amplitude of the positive peaks, indicated by vertical arrows in the figure, increases as the inter-electrode distance decrease. Estimation by exponential dependence decay gives damping length $1.4 \mu\text{m}$. It is comparable the inter-electrode distance and slightly smaller than transport length (EMFP). The latter is explained by significant influence of large angle electron scattering as found from the data of Fig. 1(c). Estimation of the cyclotron radius gives $1.4 (\text{T}\mu\text{m})/B(\text{T})$, which is two times smaller than mean radius and corresponds to the smallest horde of Electron Jack valley of molybdenum.

1.2. Hall and bend resistances

We investigated cross type W (100) nanostructures of 300 nm width and 90 nm thick. Schematic drawing is shown in Fig. 3 (left). The scale parameters for the resistance and the magnetic field are defined as $R_0 = 90 \text{ m}\Omega$ and $B_0 = 10 \text{ T}$. Hall resistance has been measured using 1,3 connections as potential leads and 2, 4 — as current leads. It shows (Fig. 3 (right), curve (1)) quasi-linear dependence at B/B_0 larger than 0.2, indicated by vertical arrow B_b . Under lowering magnetic field it decreases faster (quenching) approximately as B in power 3 and near $B_a/B_0 = 0.025$ twice crossing zero. These two characteristic points are related to the following cyclotron radii $R_b = 5 \text{ w}$ and $R_a = 40 \text{ w}$, respectively. Corresponding electron trajectories (a and b) are shown in the schematic drawing. Electrons may scatter by the corner of the cross and pass to the negative potential (3), as shown for trajectory *a*. It may cause the change of the sign of the Hall resistance at low magnetic field (point Ba in the left drawing). Electron trajectory *b* possesses the skip smaller (under

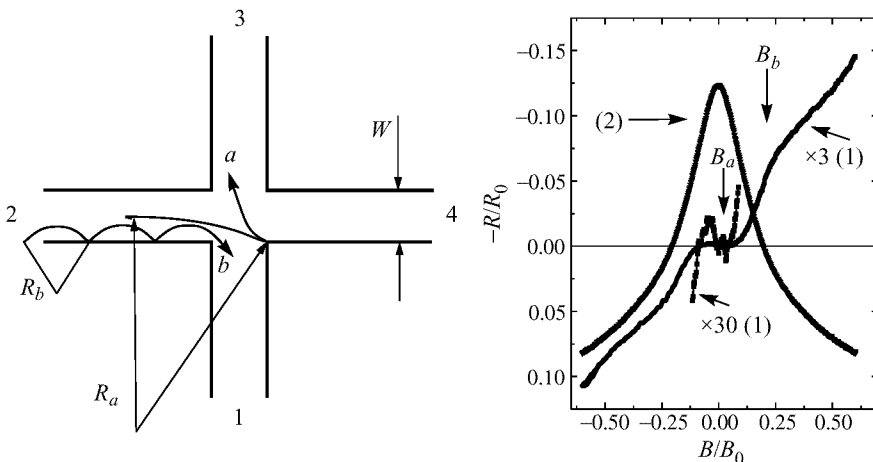


Fig. 3. Schematic drawing (left) and Hall (1) and bend (2) magnetoresistances (right).

magnetic field increase) than the lead width, while it does not at lower magnetic field. It changes a dependence of transmission probability of electrons to pass straight (from 2 to 4) or turn to the right (from 2 to 1) as a function of magnetic field. If electron flow is collimated at $B < B_b$ the Hall resistance is quenched. For the bend resistance measurements we used 1, 2 connections as a current leads and 4, 3 as a potential. Bend magnetoresistance is negative at low magnetic field and cross zero near the point B_b . For this reason, we explain its suppression by b type electron trajectory — skipping orbit, which suppress forward transmission probability under magnetic field increase.

Conclusion

We found that the normal-to-plane magnetoresistance of planar metallic single crystalline nanostructures exhibit specific for ballistic transport attributes such as transverse magnetic focusing, suppression of Hall resistance (quenching Hall effect) and negative bend resistance at moderate magnetic fields.

Acknowledgements

The work was supported by Physics of solid state nanostructures program (grant 99-1126), RFBR (grant 00-02-16601) and INTAS (grant 99-193).